Protein Science (1997), 6:13–23. Cambridge University Press. Printed in the USA.

Structure of the β_2 homodimer of bacterial luciferase from *Vibrio harveyi*: X-ray analysis of a kinetic protein folding trap

JAMES B. THODEN,[1] HAZEL M. HOLDEN,[1] ANDREW J. FISHER,[1] JAMES F. SINCLAIR,[2,3] GARY WESENBERG,[1] THOMAS O. BALDWIN,[2] AND IVAN RAYMENT[1]

[1]Institute for Enzyme Research and Department of Biochemistry, University of Wisconsin, Madison, Wisconsin 53705
[2]Department of Biochemistry and Biophysics and Center for Macromolecular Design, Texas A&M University, College Station, Texas 77843-2128

(RECEIVED October 22, 1996; ACCEPTED November 22, 1996)

Abstract

Luciferase, as isolated from *Vibrio harveyi*, is an $\alpha\beta$ heterodimer. When allowed to fold in the absence of the α subunit, either in vitro or in vivo, the β subunit of the enzyme will form a kinetically stable homodimer that does not unfold even after prolonged incubation in 5 M urea at pH 7.0 and 18 °C. This form of the β subunit, arising via kinetic partitioning on the folding pathway, appears to constitute a kinetically trapped alternative to the heterodimeric enzyme (Sinclair JF, Ziegler MM, Baldwin TO. 1994. Kinetic partitioning during protein folding yields multiple native states. *Nature Struct Biol 1*: 320–326). Here we describe the X-ray crystal structure of the β_2 homodimer of luciferase from *V. harveyi* determined and refined at 1.95 Å resolution. Crystals employed in the investigation belonged to the orthorhombic space group $P2_12_12_1$ with unit cell dimensions of a = 58.8 Å, b = 62.0 Å, and c = 218.2 Å and contained one dimer per asymmetric unit. Like that observed in the functional luciferase $\alpha\beta$ heterodimer, the major tertiary structural motif of each β subunit consists of an $(\alpha/\beta)_8$ barrel (Fisher AJ, Raushel FM, Baldwin TO, Rayment I. 1995. Three-dimensional structure of bacterial luciferase from *Vibrio harveyi* at 2.4 Å resolution. *Biochemistry 34*: 6581–6586). The root-mean-square deviation of the α-carbon coordinates between the β subunits of the hetero- and homodimers is 0.7 Å. This high resolution X-ray analysis demonstrates that "domain" or "loop" swapping has not occurred upon formation of the β_2 homodimer and thus the stability of the β_2 species to denaturation cannot be explained in such simple terms. In fact, the subunit:subunit interfaces observed in both the β_2 homodimer and $\alpha\beta$ heterodimer are remarkably similar in hydrogen-bonding patterns and buried surface areas.

Keywords: bacterial luciferase; bioluminescence; protein folding; X-ray crystallography

It has been over three decades since Christian Anfinsen and colleagues discovered that the information dictating the native fold of a protein is encoded in the sequence of amino acids constituting the polypeptide chain (Epstein et al., 1963; Anfinsen, 1973). Since that time, a large amount of data has accumulated in support of the so-called thermodynamic hypothesis: the conclusion that the native form of a protein resides at the global minimum of free energy is virtually axiomatic in the field of protein folding. In recent years, however, several examples of kinetic control in protein folding have been described (Gething et al., 1986; Waddle et al., 1987; Sugihara & Baldwin, 1988; Baker et al., 1992; Mottonen et al., 1992; Baker & Agard, 1994). For example, in the folding of bacterial luciferase, it appears that the distribution of products is determined by the relative rates with which the products form, rather than by their relative stabilities (Sugihara & Baldwin, 1988; Baldwin et al., 1993; Clark et al., 1993; Sinclair et al., 1993; Ziegler et al., 1993; Sinclair et al., 1994); this particular characteristic constitutes the definition of kinetic control.

Bacterial luciferase is particularly well suited for studies of protein folding and oligomer assembly for a variety of reasons. One question of interest that may be investigated with a heterodimeric enzyme like bacterial luciferase pertains to the effects of assembly on the structure of the protomers. For example, prior to the assembly reaction, do the individual subunits fold autonomously into their native states and then assemble into the final heterodimeric form? Or do they form partially folded species which then require a cooperative interaction to complete the assembly process? In the case of bacterial luciferase, whose functional form is an $\alpha\beta$ dimer, it is apparent that successful assembly of the enzyme requires both

Reprint requests to: Ivan Rayment, Institute for Enzyme Research, 1710 University Avenue, Madison, Wisconsin 53705; email: ivan@enzyme.wisc.edu. Address correspondence regarding the structure to Ivan Rayment and protein folding to Thomas O. Baldwin.

A preliminary report of this structure was given at the 12th International Symposium on Flavins and Flavoproteins held on June 30–July 6, 1996 in Calgary, Alberta, Canada (Baldwin et al., 1997).

[3]Present address: Johns Hopkins School of Medicine, Department of Biological Chemistry, 725 N. Wolfe St., Baltimore, Maryland 21205.

subunits to fold within the same cellular compartment, suggesting that the heterodimerization reaction involves intermediates on the folding pathway; the fully folded subunits do not combine to form the heterodimer without prior denaturation and refolding within the same solution (Waddle et al., 1987). Clearly, this protein provides a robust system for understanding the folding and assembly reactions of multimeric proteins since it has a well-defined biological function that requires formation of the correct quaternary structure.

Bacterial luciferase is a flavin monooxygenase catalyzing the bioluminescence reaction in luminous bacteria where $FMNH_2$ and an aliphatic aldehyde are oxidized by O_2 to yield the carboxylic acid, FMN, and blue-green light ($\lambda max \sim 495$ nm). Unlike most flavoenzymes, luciferase has no tightly bound flavin prosthetic group; rather, the enzyme binds reduced flavin as a substrate and releases the oxidized flavin as a product. The enzyme from *V. harveyi* is a heterodimer consisting of two homologous subunits, α and β, with molecular weights of 40,108 (355 amino acid residues) and 36,349 (324 amino acid residues), respectively (Cohn et al., 1985; Johnston et al., 1986). The amino acid sequence similarity between the two subunits is high; 80% of the residues in the β monomer are either identical or chemically similar to the corresponding residues in the α subunit (Baldwin & Ziegler, 1992). For reviews of the bacterial luciferase system, see Ziegler & Baldwin (1981) and Baldwin & Ziegler (1992). The three-dimensional structure of bacterial luciferase from *V. harveyi* reveals that each subunit in the heterodimer consists primarily of an eight-stranded $(\alpha/\beta)_8$ barrel similar to that observed in many glycolytic enzymes (Farber & Petsko, 1990; Fisher et al., 1995). As expected from the high degree of amino acid sequence similarity between the α and β subunits of luciferase (Cohn et al., 1985; Johnston et al., 1986; Baldwin et al., 1989), the overall folds of both subunits are essentially identical. The major difference is an additional loop in the α subunit that corresponds to an apparent deletion of residues 258 to 286 (relative to the α subunit) in the β subunit sequence (Baldwin et al., 1989; Baldwin & Ziegler, 1992). This similarity is also expressed by the presence of an approximate local two-fold rotational axis of symmetry that relates the α and β subunits to each other in the heterodimer (Fisher et al., 1995; Fisher et al., 1996).

The bacterial enzyme has a single active site that genetic, biochemical, and structural studies suggest is located primarily if not exclusively on the α subunit. However, both isolated α and β subunits are able to support an extremely weak bioluminescence reaction with an efficiency ca. 10^{-6}-fold less than that of the wild-type enzyme (Waddle & Baldwin, 1991; Sinclair et al., 1993; Choi et al., 1995). Although the exact role of the β subunit is unknown, it is essential for the high quantum efficiency of the enzyme, as was shown originally for the luciferase from *Vibrio fischeri* (Friedland & Hastings, 1967) and as has since been found for the luciferases from other bacterial species as well.

The folding pathway for bacterial luciferase has been extensively characterized. Expression of the individual subunits of *V. harveyi* luciferase from recombinant plasmids in *Escherichia coli* resulted in the accumulation of large amounts of soluble protein in the cell lysates (Waddle et al., 1987), demonstrating that the individual subunits fold in vivo to yield stable, soluble entities. When cell lysates containing the individual subunits were mixed under nondenaturing conditions, however, the native enzyme did not form. Denaturation of the mixed cell lysates followed by dilution of the denaturant to allow refolding resulted in the formation of large amounts of active luciferase, suggesting that the correct assembly of the native enzyme involves interactions between partially folded subunits (Waddle et al., 1987). Subsequently, it was shown that the purified native subunits likewise were unable to assemble in vitro into the active heterodimer without prior unfolding (Baldwin et al., 1993; Sinclair et al., 1993). Thus, it appears that formation of the active heterodimer requires both subunits to fold within the same cellular compartment at the same time. On the basis of these observations, Waddle et al. (1987) suggested that in vivo the subunits must interact as partially folded species and that the final steps of folding must occur within the heterodimeric species. These observations raised the possibility that formation of the biologically active heterodimer might be kinetically controlled, since the "completely" folded individual subunits do not associate upon mixing, even after prolonged incubation. In related experiments, Sugihara and Baldwin (1988) described deletion mutations in the C-terminal region of the β subunit of luciferase that resulted in a dramatic reduction in the efficiency with which the mutant β subunit combined with the α monomer to yield luciferase; however, when folded these enzymatically active, truncated mutants displayed normal thermal stability. These experiments supported the idea that the assembly of the enzyme may be under kinetic control, and suggested that the C-terminal region of the β subunit might play some type of role in stabilizing the transition state in the assembly reaction.

The original report of Friedland and Hastings (1967) that bacterial luciferase from the species *V. fischeri* was built from two nonidentical subunits suggested that the α subunit, when refolded separately from the β subunit, retained its ability to form an active enzyme when combined with β, whereas the separately folded β subunit formed an inactive oligomeric structure. More recent studies on the folding of the enzyme from *V. harveyi* have demonstrated that both the α and β subunits fold into stable, globular structures with well-defined tertiary motifs that, by spectroscopic methods, appear similar to the folds they assume in the heterodimer (Sinclair et al., 1993; Sinclair et al., 1994). The folded α subunit appears fully competent to interact with the folding β subunit (Fedorov & Baldwin, 1995) but the β subunit forms a homodimer with a second order rate constant of approximately 180 $M^{-1} \cdot s^{-1}$ at 18 °C in 50 mM phosphate (pH 7.0) (Sinclair et al., 1994). The dissociation rate constant for the homodimer is approximately 10^{-14} s^{-1} under the same conditions, which explains the earlier observation that mixtures of the two subunits do not form native $\alpha\beta$ luciferase. There is a significant kinetic barrier between the monomeric and homodimeric forms of the β subunit, in sharp contrast to the folding of the heterodimeric enzyme. In 5 M urea, the β_2 species maintains its native tertiary structure as indicated by near ultraviolet circular dichroism; unfolded β subunit in 5 M urea (obtained from $\alpha\beta$ luciferase, which is rapidly unfolded in 5 M urea) remains unfolded indefinitely. The hysteresis in the unfolding and refolding transitions indicates that in the range of 2–6 M urea, the 2β to β_2 reaction does not attain equilibrium even following prolonged incubation (Sinclair et al., 1994), whereas the $\alpha\beta$ species achieves equilibrium under these conditions comparatively quickly (Clark et al., 1993). Interestingly, the thermodynamic stability of the β_2 homodimer is about the same as that of the $\alpha\beta$ protein.

It has been demonstrated that the final distribution of the products in the folding of the bacterial luciferase is determined by the relative rate constants of the various steps on the kinetic pathway of assembly for the $\alpha\beta$ and β_2 species (Sinclair et al., 1994). The luciferase β subunit either assembles with an α subunit to form the heterodimeric enzyme, or it reacts with itself to form the β_2 homo-

dimer that is kinetically inert on a biological time scale (Sinclair et al., 1994). In order to develop an understanding of the structural basis for the kinetic stability of the β_2 homodimer, we have crystallized and determined its molecular structure to 1.95 Å resolution. In combination with detailed kinetic and thermodynamic studies (Sugihara & Baldwin, 1988; Baldwin et al., 1993; Clark et al., 1993; Sinclair et al., 1993; Ziegler et al., 1993; Sinclair et al., 1994) and the high resolution structure of the $\alpha\beta$ heterodimer (Fisher et al., 1996), this X-ray analysis provides a unique opportunity to investigate the structural basis of a slow process in protein folding.

Results

Overall structure of the β_2 homodimer

A ribbon representation of the homodimer of the β subunit of bacterial luciferase is shown in Figure 1. Electron density is visible for Met 1 to His 323 in Subunit 1 and Met 1 to Ser 324 in Subunit 2. The connectivity of the electron density is unambiguous. The homodimer has overall dimensions of 70 Å × 76 Å × 70 Å and as expected, each subunit contains nine strands of parallel β sheet and 12 major α-helices. The two subunits constituting the dimer are very similar such that all backbone atoms from Met 1 to His 323 superimpose with a root-mean-square deviation of 0.69 Å and are related to one another by a rotation of 179.5 degrees which within experimental error is an exact twofold axis of rotation. There are four surface loops, however, where the polypeptide chains for the two subunits adopt slightly different conformations. These regions are delineated by Cys 108 to Phe 125, Cys 144 to Lys 155, Gln 213 to Gln 221, and Glu 253 to Asp 259. In both subunits, the backbone atoms residing in the loop formed by Glu 253 to Asp 259 display significantly higher temperature factors, implying conformational flexibility. With respect to the other three surface loops, the electron density is better defined for these secondary structural elements in Subunit 2. The two subunits of the β_2 homodimer also differ at the C-terminus beginning at Ala 317. Excluding these above-mentioned residues, the backbone atoms for the two subunits in the β_2 homodimer superimpose with a root-mean-square deviation of 0.30 Å.

There are two parallel α-helices in each monomer, delineated by Pro 55 to Gly 64 and Pro 83 to Met 96, that provide the major structural framework for the subunit:subunit interface. In addition, there is a random coil region between Val 41 and Pro 55 that provides both electrostatic and hydrophobic interactions for further stabilization of the quaternary structure. The surface area lost upon dimer formation is approximately 3970 Å^2 when computed with a probe of radius 1.4 Å and the algorithm of Lee and Richards (1971) as implemented in EDPDB (Zhang & Matthews, 1995).

The average B-value for the waters is 49.1 Å^2. Of the 989 water molecules located in the electron density map, 25 have temperature factors below 20.0 Å^2. Many of these solvents link side-chain functional groups with polypeptide chain backbone atoms. Some play more important structural roles by serving as bridges between secondary structural elements. For example, in each subunit there is a well-ordered water molecule located within hydrogen-bonding distance of O of Leu 8, O of Tyr 42, and N of Val 52, which serves to stabilize the polypeptide chain backbone near β-strands 1 and 2. Nine of these very well-ordered waters are located in or near the subunit:subunit interface.

Comparison of the β_2 homodimer and the $\alpha\beta$ heterodimer

The overall fold of the β subunit in the homodimer is nearly identical to that observed for the β subunit in the $\alpha\beta$ heterodimer

Fig. 1. Ribbon representation of the β_2 homodimer of bacterial luciferase. Subunit 1 is shown in blue and green while Subunit 2 is depicted in red and yellow. The local two-fold rotational axis relating the two subunits in the dimer is located at the center of the figure and lying perpendicular to the plane of the page. The subunit:subunit interface is formed by amino acid residues residing in primarily α-helical regions. The four surface loops that differ in conformation between the two subunits are shown in white, whereas the putative vestigial active site for Subunit 1 that lies at the C-terminal end of the β-barrel is indicated by the arrow. Figures 1-4 were prepared with the program MOLSCRIPT (Kraulis, 1991).

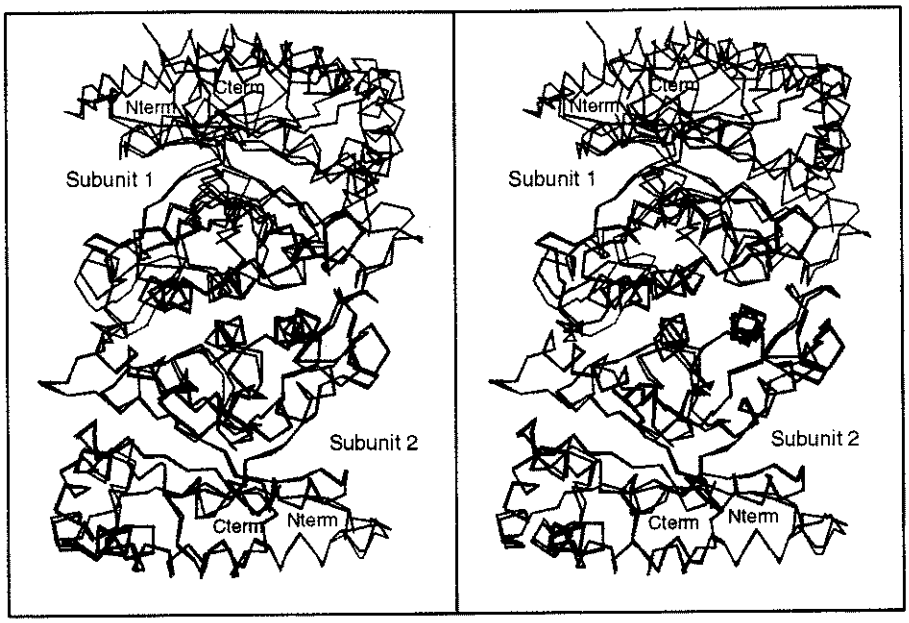

Fig. 2. Comparison of the α-carbon traces for the β_2 and the $\alpha\beta$ dimers. The coordinates for the $\alpha\beta$ heterodimer refined at 1.5 Å resolution (Brookhaven Protein Data Bank accession number 1LUC (Bernstein et al., 1977)) were used for the comparison (Fisher et al., 1996). The β subunit of the $\alpha\beta$ heterodimer was oriented onto Subunit 2 of the homodimer with the program LSQKAB written by Kabsch and implemented in (CCP4 1994). The β subunits for the homodimer, depicted in black, have been labeled 1 and 2. The α and β subunits of the heterodimer are displayed in red and green, respectively.

as shown in Figure 2. The root-mean-square differences between the various subunits in the homo- and heterodimers are given in Table 1. As evident from Figure 2, when the β subunits of the homo- and heterodimers are superimposed there is a small difference in the rotational angle (4 degrees) between the remaining α and β subunits. For all of the structural comparisons the coordinates from the high resolution structure determination of the $\alpha\beta$ heterodimer at 1.5 Å were used (Fisher et al., 1996). Interestingly, the root-mean-square deviations between the α-carbon coordinates for Subunits 1 and 2 of the β_2 homodimer are the same as those for either subunit in the homodimer and the β subunit in the heterodimer. These data demonstrate that, within experimental error, the β subunit adopts the same conformation in both oligomeric states.

Figure 2 shows the remarkable coincidence between the secondary structural elements that provide the interfaces for the $\alpha\beta$ hetero- and the β_2 homodimers, particularly in the α-helical bundle that forms the core of the subunit:subunit interaction. This is not surprising, however, given the amino acid sequence similarity between the α and β subunits at the interface. The major differences between the β_2 homodimer and $\alpha\beta$ heterodimer occur away from the interface in the surface regions formed by Val 31 to Lys 35, Glu 109 to Asp 113, Asn 118 to Gln 124, Asp 195 to Ala 199, and Glu 248 to Glu 266.

As expected, there are similarities in the hydrogen-bonding pattern within the molecular interface. A list of the hydrogen bonds formed between side-chain functional groups and main-chain backbone atoms at the interface of the β_2 homodimer is given in Table 2. Water-mediated hydrogen bonds in the subunit:subunit interface are listed in Table 3. Included in Tables 2 and 3 is an indication of the equivalent hydrogen bonds found in the $\alpha\beta$ heterodimer. A total of 22 intersubunit hydrogen bonds and 45 water-mediated interactions was identified in the $\alpha\beta$ heterodimer of bacterial luciferase (Fisher et al., 1996). In contrast, 16 and 30 intersubunit and water-mediated interactions, respectively, are observed in the β_2 homodimer interface. Most of the intersubunit hydrogen bonds occur in symmetry-related pairs, reflecting the local two-fold rotational axis that relates the two β subunits. This is particularly true for the buried hydrogen bonds. Deviations from dyad symmetry are found at the extremities of the dimeric interface between loops whose conformations appear to be influenced by crystal packing forces. For example, both Ser 17 and Phe 116 are located at the edge of the interface. Most of the amino acid residues participating in hydrogen-bonding at the subunit:subunit boundary are located in secondary structural elements other than the central bundle of α-helices. Although there appear to be substantially fewer hydrogen bonds in the β_2 homodimer, this is somewhat misleading due to the large number of interactions in the secondary coordination sphere just beyond the cutoff of 3.2 Å, such that it is difficult to interpret the effect of the hydrogen bonds on the thermodynamic and kinetic stability of these species.

Table 1. *Root-mean-square differences measured in Å between the structurally equivalent atoms in the α and β subunits of the luciferase homo and heterodimers*

	α/β heterodimer, α subunit	α/β heterodimer, β subunit	β_2 homodimer, Subunit 2
β_2 homodimer, Subunit 1	6.2[a] (6.0)[b]	0.7 (1.2)	0.63 (1.1)
β_2 homodimer, Subunit 2	6.2 (6.0)	0.6 (1.1)	

[a]For α-carbon atoms only.
[b]For structurally equivalent α-carbons.

Table 2. *Intersubunit hydrogen bonds in the β_2 homodimer and the equivalent interactions in the $\alpha\beta$ heterodimer*

Subunit 1		Subunit 2		Bond Distance (Å)	α subunit	
Residue	Atom	Residue	Atom		Residue	Atom
Ser 17	O^{γ}	His 161	$N^{\delta 1}$	3.0	[b]	
Asp 18[a]	$O^{\delta 1}$	Gln 95	$N^{\epsilon 2}$	2.7	Thr 18	O^{γ}
Asp 18[a]	$O^{\delta 1}$	Gln 95	$O^{\epsilon 1}$	3.2	Thr 18	O^{γ}
His 45[a]	$N^{\delta 1}$	Glu 88	$O^{\epsilon 1}$	2.7	His 45	$N^{\delta 1}$
His 45[a]	$N^{\delta 1}$	Glu 88	$O^{\epsilon 2}$	3.3	His 45	$N^{\delta 1}$
Thr 80[a]	O	Arg 85	$N^{\eta 2}$	2.9	Thr 80	O
Thr 80[a]	O^{γ}	Arg 85	$N^{\eta 2}$	2.6	Thr 80	O^{γ}
Phe 116	O	His 82	N^{ϵ}	2.6	Val 116	O
Ser 47[a]	O	Asn 159	$N^{\delta 2}$	3.1	None	

[a]The two-fold related hydrogen bonding interaction is also observed at the subunit:subunit interface for these pairs of atoms with comparable geometry and hydrogen bond distance.

[b]The equivalent side chain in the α subunit (Gln 17) forms a structurally nonequivalent hydrogen bond to the amide nitrogen of His 161.

For orientation purposes, a close-up view of the subunit:subunit interface of the β_2 homodimer, viewed down the molecular dyad, is displayed in Figure 3A. The interfacial region of Subunit 2 of the β_2 homodimer, defined by Phe 10 to Ala 162, is shown in Figure 3B. Superimposed upon this region is the polypeptide chain backbone for the β subunit of the $\alpha\beta$ heterodimer. Those side chains shown are involved in direct or water-mediated hydrogen bonding in the β_2 homodimer as listed in Tables 2 and 3. As can be seen, the side chains adopt very similar conformations whether the β subunit of bacterial luciferase is associated with either another β subunit or an α monomer.

The surface area buried at the subunit:subunit interface is similar for both the homo- and heteroproteins. Specifically, as described above, the calculated total buried surface area at the subunit:subunit interface for the β_2 homodimer is 3970 Å^2. In the native luciferase, the α and β subunits contribute 2150 Å^2 and 2100 Å^2, respectively, to the total buried surface area of 4250 Å^2. Likewise, the nature of the buried surface area is similar in both forms of the enzyme. There is a difference in the total charge on the homodimer and heterodimer as calculated with GRASP (Nicholls et al., 1991). This suggests that at pH 7 the hetero- and homodi-

Table 3. *Water-mediated intersubunit contacts*

Subunit 1	Distance (Å)	Water	Distance (Å)	Subunit 2	α/β heterodimer[a]
$N^{\eta 2}$ Arg 85	3.2	O83-809	2.7	O Val 77	++
$N^{\eta 2}$ Arg 85	3.2	O83-809	2.9	$O^{\epsilon 1}$ Gln 33	++
$N^{\eta 1}$ Arg 85	2.8	O83-809	2.9	$O^{\epsilon 1}$ Gln 33	++
$N^{\eta 1}$ Arg 85	2.8	O83-809	2.7	O Val 77	++
$O^{\epsilon 2}$ Glu 89	2.3	O87-809	3.2	$O^{\epsilon 1}$ Glu 89	+
$O^{\delta 1}$ Asn 159	3.0	O48-809	3.1	N Ser 47	−
$O^{\delta 1}$ Asn 159	3.0	O48-809	2.7	O Ser 47	−
$O^{\delta 1}$ Asn 159	3.0	O48-809	2.5	O Gly 50	−
$N^{\epsilon 2}$ His 161	2.7	O45-809	2.1	$O^{\delta 2}$ Asp 18	−
$O^{\delta 1}$ Asp 18	3.2	O54-803	3.0	O Ala 162	−
O Ala 162	2.8	O77-803	2.8	$O^{\delta 1}$ Asp 18	+
O Asn 159	2.7	O37-801	3.2	O Val 51	+
O Asn 159	2.7	O37-801	2.7	N Gly 53	+
O Gly 53	2.8	O59-800	2.9	$N^{\eta 1}$ Arg 85	+
$O^{\epsilon 1}$ Glu 89	3.4	O62-800	2.9	$O^{\epsilon 2}$ Glu 89	+
$O^{\epsilon 1}$ Glu 89	3.4	O62-800	3.1	O^{γ} Thr 57	+
N^{ϵ} Arg 85	2.9	O79-800	2.9	O Thr 80	+
N Gly 53	2.7	O57-800	2.8	O Asn 159	+
O Val 51	3.5	O57-800	2.8	O Asn 159	+
N Phe 46	2.7	O48-800	2.7	$O^{\epsilon 1}$ Glu 88	+
N Phe 46	2.7	O48-800	3.5	O Asn 159	+
N Phe 46	2.7	O48-800	3.3	N Asn 159	+
O Ser 47	2.9	O47-800	3.3	N Asn 259	+
N Ser 47	3.0	O47-800	3.3	N Asn 159	+
O^{γ} Thr 80	3.0	O78-800	3.1	$N^{\eta 2}$ Arg 85	+
O^{γ} Thr 80	3.0	O78-800	2.6	$N^{\eta 1}$ Arg 85	+
O Val 77	2.9	O78-800	3.1	$N^{\eta 2}$ Arg 85	+
O Val 77	2.9	O78-800	2.6	$N^{\eta 1}$ Arg 85	+
$O^{\epsilon 1}$ Glu 43	2.6	O78-800	3.1	$N^{\eta 2}$ Arg 85	+
$O^{\epsilon 1}$ Glu 43	2.6	O78-800	2.6	$N^{\eta 1}$ Arg 85	+

[a]++, Water is located in an identical position; +, water is located within 0.5 Å of the equivalent position; −, no equivalent water molecule is observed in the $\alpha\beta$ heterodimer.

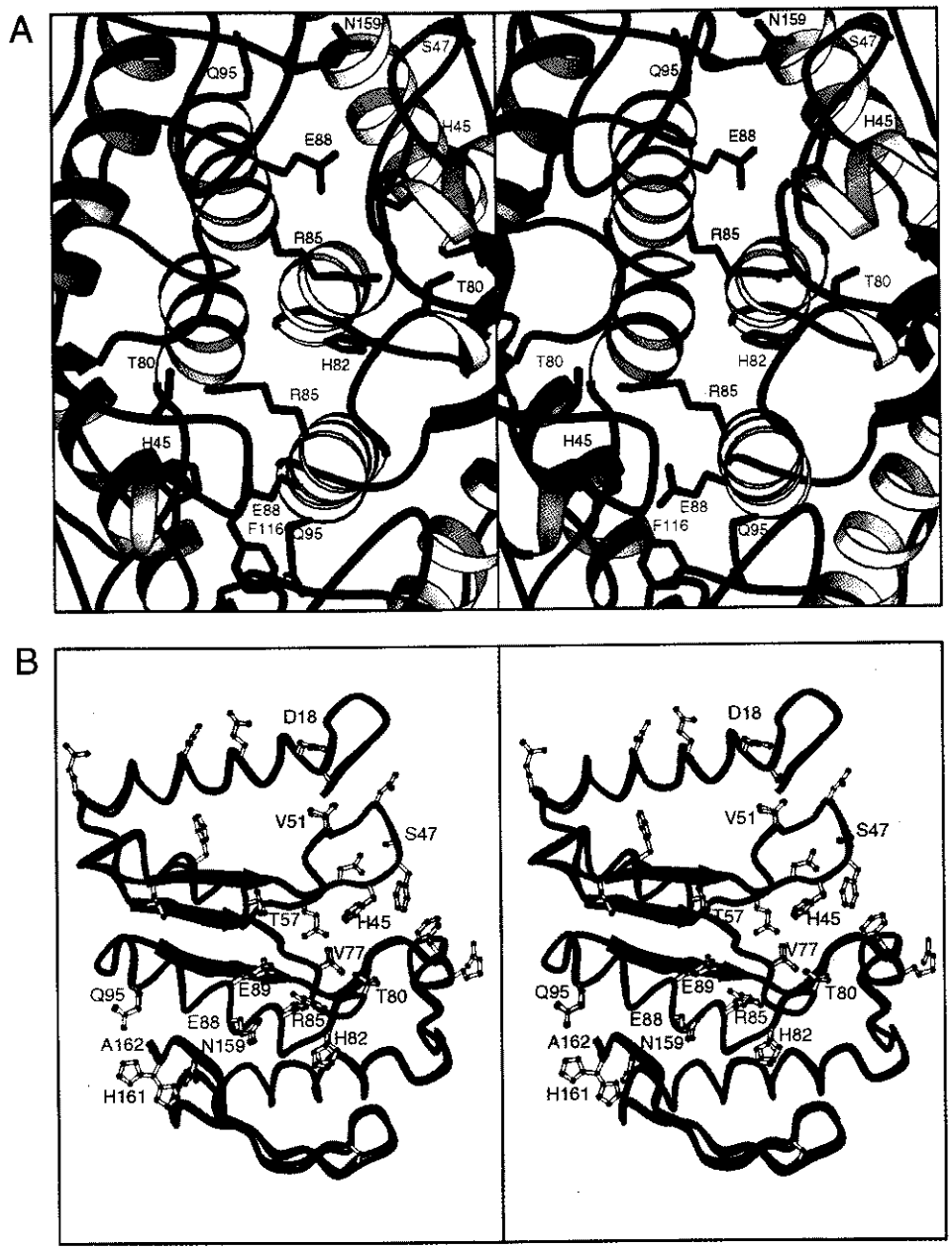

Fig. 3. Stereo view of those amino acid residues important in subunit:subunit hydrogen bonding. **A:** A close-up view of the molecular interface for the β_2 homodimer of luciferase is shown. Those secondary structural elements from Subunit 1 are depicted in blue and green; those from Subunit 2 are shown in red and yellow. Several of the amino acid residues involved in intersubunit hydrogen bonding are displayed in ball-and stick representations. The molecular two-fold rotational axis is perpendicular to the plane of the page. **B:** Shown here is the dimer interface contributed by Subunit 2. The figure is oriented such that the molecular dyad of the dimer lies in the plane of the page and the top portion of Subunit 2, as shown in **A**, is located at the right hand side of the page. The polypeptide chain backbone from Subunit 2 of the β_2 homodimer is shown in red. The β subunit from the $\alpha\beta$ heterodimer is depicted in blue. Those side chains that form intersubunit and water-mediated hydrogen bonds are displayed in ball-and-stick representations. Only those side chains that adopt slightly different conformations between the two β subunits are labeled. The electron density for His 161 in Subunit 2 of the β_2 homodimer shows two alternative conformations for the imidazole ring as indicated.

mers carry a net negative charge of -37 and -32, respectively, and that some of the charge differences are associated with the interface. Typically, the overall charge on a protein does not correlate well with the protein stability, although it might influence the kinetic barrier for unfolding.

One of the striking features of the quaternary structures of both the $\alpha\beta$ heterodimer and β_2 homodimer is a large solvent pocket that lies at the interface between the subunits. As seen in Figures 4A and B, this region is very similar in both molecules and contains a similar distribution of water molecules. Although more solvents are observed in the $\alpha\beta$ heterodimer, this most likely results from the higher resolution of its structural analysis. Overlap of the water molecules in the $\alpha\beta$ heterodimer onto the $(F_o\text{-}F_c)$ electron density for the β_2 homodimer reveals weak density for

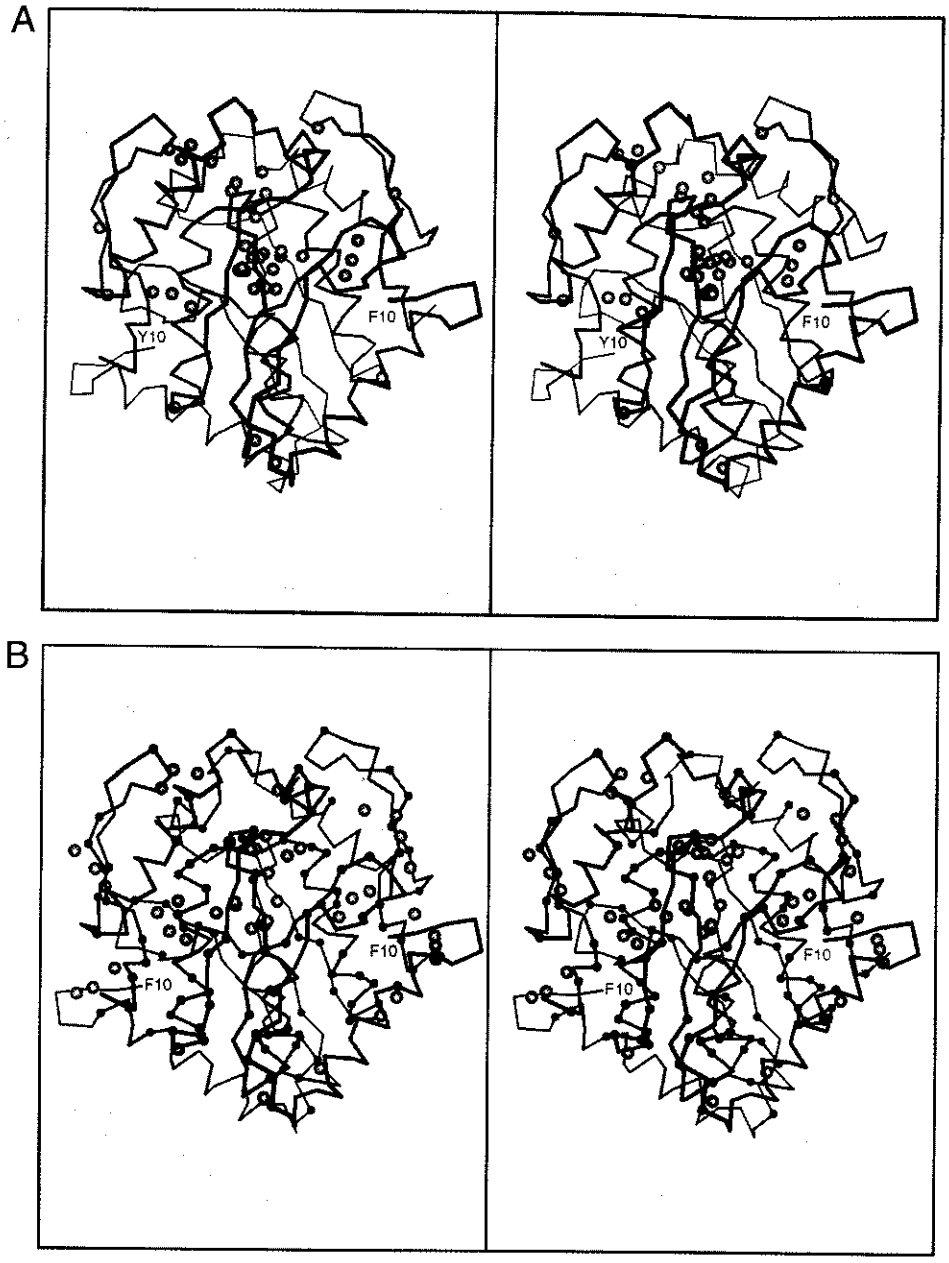

Fig. 4. Close-up view of the buried water molecules that lie at the interface of the $\alpha\beta$ heterodimer and β_2 homodimer. α-carbons 10 to 165 are shown. The water pocket is located above the four helix bundle that forms the core of the protein-protein interface. **A:** $\alpha\beta$ heterodimer where the α and β subunits are depicted in red and blue, respectively. **B:** β_2 homodimer where Subunits 1 and 2 are shown in red and blue, respectively. **B** also marks the location of the identical residues in the sequences of the α and β subunits as small spheres.

those apparently omitted from the structure of homodimer. This further confirms that the water structure is very similar in both structures. It appears that there is very similar accessibility to the pocket by solvent molecules in both proteins. Figure 4B also shows the location of the identical residues in the α and β subunits mapped onto the β_2 homodimer. The overall amino acid sequence identity between the α and β subunits is ~36%; however, as can be seen, many of the residues located in the interface are conserved. Given the similarity between the solvent pockets, the large difference in activation energy for the unfolding of the $\alpha\beta$ heterodimer and β_2 homodimer (Sinclair et al., 1994) cannot be ascribed to any obvious differences in the accessibility. However, this does not preclude the possibility that solvent accessibility is an important determinant of kinetic stability, only that it is difficult to identify the nature of this from the present X-ray models.

Discussion

There are two fundamental issues concerning the structure of the β_2 homodimer. Of lesser global significance is the fact that the β_2 homodimer exhibits a very small but measurable bioluminescence activity (Waddle & Baldwin, 1991; Sinclair et al., 1993). This observation has been challenged (Li et al., 1993), but more recently the activity of the β subunits has indeed been confirmed (Choi

et al., 1995). Since the active center of luciferase resides on the α subunit, it is not especially surprising that the free α monomer has some residual activity. Furthermore, since the α and β subunits display great structural similarity on both the primary and tertiary level, it is also not surprising that the β subunit retains some vestigial aspects of an active center. The bioluminescence yield from the free β subunits is so weak, however, that the three-dimensional structure of the β_2 homodimer can hardly be expected to yield much basic knowledge regarding the catalytic activity of luciferase.

The second issue, on the other hand, pertains to the structural basis of slow conformational changes in proteins. The β_2 homodimer forms slowly, and dissociates under nondenaturing conditions exceedingly slowly. To explain the striking difference in behavior between the β_2 homodimer and the $\alpha\beta$ heterodimer, which unfolds very rapidly in 5 M urea, it was expected that some type of domain swapping would be observed in the structure of the β_2 homodimer. As shown in this X-ray structural analysis, however, the two β subunits associate together in a nearly identical arrangement to that observed in the native bacterial luciferase. Careful examination of the subunit interface regions shows that no secondary structural elements of one subunit of the β_2 homodimer have been exchanged with the other. Furthermore, the two subunits have an extensive, relatively flat interface, with no significant excursions of one subunit into its neighbor. It should be stressed that the stability of the β_2 homodimer in 5 M urea is a kinetic rather than a thermodynamic phenomenon. The thermodynamic driving force in the presence of 5 M urea strongly favors the unfolded state of the subunit but, kinetically, the β_2 homodimer cannot unfold on a reasonable time scale. At higher urea concentrations, the β_2 homodimer does unfold but, upon dilution of the urea, the protein remains unfolded and does not show any tendency to refold and dimerize until the denaturant concentration is reduced below 1 M (Sinclair et al., 1994). Knowledge of the high resolution X-ray structure of the β_2 homodimer is exceedingly important for unraveling the details of this important and poorly understood phenomenon. Yet, from this study, it is also apparent that the three-dimensional structure alone cannot fully indicate the nature of the forces that prevent the β_2 homodimer from unfolding. To fully appreciate the molecular basis of this slow structural rearrangement, a better understanding of the three-dimensional architectures of the subunits, as they begin to interact to form the dimeric species, must be obtained.

The associations and disassociations of the β_2 and the $\alpha\beta$ species of bacterial luciferase are excellent examples of the importance of kinetic factors in protein assembly. They show that a kinetic barrier for a conformational change can prevent the process from occurring, even when, thermodynamically, the change is greatly favored. From the structure presented here, it is apparent that kinetic barriers, as well as the more basic thermodynamic parameters, are difficult to explain at the molecular level, even when high resolution X-ray crystallographic structures are available.

Materials and methods

Materials

DEAE Sephadex A-50 was purchased from Sigma, Ultrogel AcA 54 from IBF Biotechnics, 1,3-Bis[tris-(hydroxymethyl)methylamino]propane (BTP) from Aldrich, dithiothreitol from Boehringer Mannheim Biochemicals, EDTA from Research Organics, polyethylene glycol-3400 (PEG) from Aldrich, FMN from Calbiochem, and UltraPure urea from Schwartz-Mann. All inorganic salts were purchased from Baker or Fisher and were of the highest purity grade available.

Plasmid construction, bacterial growth, and cell lysis

E. coli strain BL21 (Novagen) was employed for the overexpression of the recombinant *V. harveyi luxB* gene. Plasmid pbT7, encoding the luciferase β subunit from *V. harveyi* under control of the T7 promoter of pT7-6 was constructed by inserting the Pst1-Sac1 fragment carrying a fragment of *luxA*, all of *luxB*, and a fragment of *luxE* from pTB7 (Baldwin et al., 1984) into pT7-6 that had been opened by Pst1 and Sac1. The medium used was LB supplemented with ampicillin (100 μg/mL). Cells were grown at 22 °C in 2.7 liter Fernbach flasks containing 1.5 liter medium in air bath shakers with agitation at 250 rpm. At an OD_{600nm} of about 0.8, the T7 polymerase was induced by addition of 5 mM lactose. When the cells had reached OD_{600nm} of 4–5, they were harvested by centrifugation, lysed with a French pressure cell, and the β subunit purified as described (Sinclair et al., 1993). Under these growth conditions, most of the β subunit was soluble. However, at higher temperatures, most of the β subunit was found in the insoluble fraction, as described earlier (Waddle & Baldwin, 1991; Sinclair et al., 1993).

Crystallization conditions

Three different crystal forms of the β_2 homodimer were obtained. For the first form, 10 μL of protein, at a concentration of 20–25 mg/mL (as determined from an extinction coefficient of 0.71 $(mg/mL)^{-1}\cdot cm^{-1}$ (Sinclair et al., 1993)) in 100 mM phosphate (pH 7.0), 1 mM EDTA, and 0.5 mM dithiothreitol were mixed with 10 μl of a solution containing 1.5 M ammonium sulfate, 250 mM sodium borate, and 50 mM succinic acid (pH 8.5). These droplets were subsequently placed on silanized glass coverslips and allowed to equilibrate against the 1.5 M ammonium sulfate solution by the hanging drop method of vapor diffusion. Diamond-shaped crystals generally appeared within 24 h, and reached maximum dimensions of 1.5 mm × 0.5 mm × 0.5 mm after one week. These crystals belonged to the orthorhombic space group $P2_12_12_1$ with unit cell dimensions of a = 61.4 Å, b = 61.5 Å, and c = 227.2 Å as determined by precession photography. An initial X-ray data set was collected from one crystal to 2.6 Å resolution at 4 °C. These crystals were stable in the X-ray beam for 24–36 h. Since this crystal form diffracted to better than 2.0 Å resolution, attempts were made to obtain a higher resolution X-ray data set from multiple crystals. Unfortunately, X-ray data collected from several crystals would not merge together satisfactorily. An additional attempt was made to collect the X-ray data at cryogenic temperatures from a single crystal transferred to a solution containing 1.75 M ammonium sulfate and 25% ethylene glycol. Although several high quality X-ray data sets, as judged from the scaling statistics, were collected from single crystals to 2.0 Å resolution at −150 °C, the resulting electron density maps were of poor quality.

As a consequence, a search for new crystallization conditions was initiated. With the use of a sparse matrix screen, crystals isomorphous to the ammonium sulfate form were produced from sodium/potassium phosphate, ammonium phosphate, sodium citrate, sodium/potassium tartrate, or polyethylene glycol (PEG) 3400. Based on the previous problems encountered with crystals grown from salt (ammonium sulfate), the PEG conditions were further explored. In addition to the diamond-shaped crystals from PEG 3400, a second hexagonal rod-like form appeared in the same

Table 4. *Intensity statistics*

	Resolution range (Å)							
	Overall	30.00–3.73	2.96	2.59	2.35	2.18	2.05	1.95
No. of measurements	125,700	26,453	25,491	20,027	16,032	1,4534	12,970	9,563
No. of independent reflections	55,442	8,300	8,082	8,158	8,168	8,000	7,861	6873
Completeness of data (%)	93.7	94.1	95.0	98.0	95.9	95.0	92.5	85.1
Average intensity	3,896	10,000	5,280	2,125	1,279	880	635	418
Average sigma	262	360	327	225	196	202	201	185
R_{factor} (%)[a]	4.1	2.7	4.5	6.7	8.2	11.6	14.0	18.0

[a] $R_{factor} = (\Sigma|I - \bar{I}|/\Sigma I) \times 100$.

drop. Precession photographs of these hexagonal rods revealed that they belonged to the space group $P6_122$ (or $P6_522$) with unit cell dimensions of approximately $a = b = 86$ Å and $c = 390$ Å. Due to the large unit cell displayed by these rods, conditions for optimizing the diamond-shaped form were subsequently investigated. It was found that with a protein concentration of 25 mg/mL and a crystallization solution containing 18–20% PEG 3400, 750 mM NaCl, and 100 mM 1,3-Bis[tris-(hydroxymethyl)methylamino]propane (BTP) (pH 7.0), large single crystals could be grown that reached maximum dimensions of 1.4 mm × 0.5 mm × 0.5 mm. These crystals generally appeared after 4–5 days, and reached their maximum size in 2–3 weeks. Like those grown from ammonium sulfate, the crystals obtained from PEG belonged to the orthorhombic space group $P2_12_12_1$ with unit cell dimensions of $a = 61.9$ Å, $b = 62.1$ Å, and $c = 225.6$ Å. These crystals diffracted to a nominal resolution of 2.0 Å, but were stable in the X-ray beam for only 12–24 h. An attempt was made to collect a complete X-ray data set from multiple crystals at 4 °C, but again these data would not merge together satisfactorily. Conditions were explored for collecting X-ray data at cryogenic temperature, but a large survey of cryoprotectants failed to yield a set of conditions where the crystals would diffract to any extent after flash-cooling in a nitrogen stream.

A closer examination of the crystallization experiments employed to optimize the crystals from PEG 3400 revealed yet a third crystal form that grew as plates. This crystal form proved difficult to reproduce, and the crystals would never grow very large. Occasionally, these crystals would appear under the following conditions: protein at 15 mg/mL, 26–30% PEG 3400, 200–300 mM NaCl, and 100 mM BTP (pH 7.0). Initially a significant amount of material would precipitate over the course of 1–2 weeks, and then after an additional 1–3 weeks the plate-like crystals would occasionally appear, reaching a maximum size of 0.3 mm × 0.2 mm × 0.075 mm. These crystals also belonged to the orthorhombic space group $P2_12_12_1$ with unit cell dimensions of $a = 58.8$ Å, $b = 62.0$ Å, and $c = 218.2$ Å, and contained one β_2 homodimer per asymmetric unit. Despite their small size, these crystals diffracted to better than 2.0 Å resolution and proved to be amenable to the introduction of cryo-protectants. This crystal form was ultimately employed in the structural determination described here.

X-ray data collection and processing

Prior to X-ray data collection, a single crystal was transferred from the hanging drop to a synthetic mother liquor containing 30% PEG 3400, 750 mM NaCl, and 100 mM BTP propane (pH 7.0). Following equilibration for 1 h, the crystal was serially transferred in three steps over 5 min to a cryo-protectant solution containing 33% PEG 3400, 900 mM NaCl, 100 mM BTP (pH 7.0), and 5% sucrose. The crystal was suspended in a thin film of the cryoprotectant solution in a loop made from 20 micron surgical thread and flash-cooled to −150 °C in a stream of nitrogen gas (Teng, 1990; Rodgers, 1994).

X-ray data were collected at −150 °C with a Siemens HI-STAR dual area detector system equipped with Supper double-focusing mirrors. The X-ray source was CuK_α radiation from a Rigaku RU200 rotating anode generator operated at 50 kV and 50 mA and equipped with a 200 μm focal cup. An entire data set was collected from a single crystal. These X-ray data were processed according to the procedure of Kabsch (Kabsch, 1988a; Kabsch, 1988b) and internally scaled with XCALIBRE (Wesenberg & Rayment, 1995). The X-ray data set was 94% complete to 1.95 Å resolution and scaled with an overall R_{sym} of 4.1%. Relevant data collection statistics are presented in Table 4.

Computational methods

The structure was solved by molecular replacement with the software package AMORE (Rossmann, 1972; Navaza, 1993). For the necessary search model, a dimer of β subunits was constructed from the β subunit of the $\alpha\beta$ luciferase solved to 2.4 Å resolution (Fisher et al., 1995). The three-dimensional model was refined by multiple cycles of manual model building with the program FRODO (Jones, 1985) and least-squares refinement with the software package TNT (Tronrud et al., 1987). Refinement statistics can be found

Table 5. *Least-squares refinement statistics for the luciferase β_2 homodimer*

Resolution limits (Å)	30.0–1.95
R_{factor} (%)[a]	18.8
No. of reflections used	55,442
No. of protein atoms	5,127
No. of solvent atoms	989
Weighted root-mean-square deviations from ideality	
Bond length (Å)	0.016
Bond angle (deg)	2.5
Planarity (trigonal) (Å)	0.007
Planarity (other planes) (Å)	0.012
Torsional angle (deg)[b]	16.9

[a] $R_{factor} = \Sigma|F_o - F_c|/\Sigma|F_o|$ where F_o is the observed structure-factor amplitude and F_c is the calculated structure-factor amplitude.
[b] The torsional angles were not restrained during the refinement.

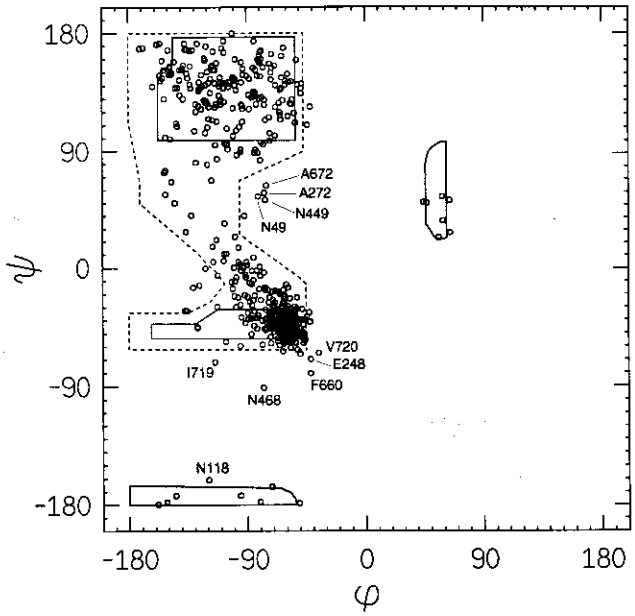

Fig. 5. Plot of the main chain dihedral angles for all non-glycinyl residues in the final model of the luciferase β_2 homodimer. Fully allowed ϕ,ψ values are enclosed by solid lines; those partially allowed are enclosed by dashed lines. In the X-ray coordinate file, residues 1 to 323 and 401 to 724 correspond to Subunits 1 and 2, respectively.

in Table 5. A Ramachandran plot (Ramakrishnan & Ramachandran, 1965) of the main chain conformational angles is displayed in Figure 5 and indicates that most of the non-glycinyl and residues lie within or very close to the allowed regions of conformational

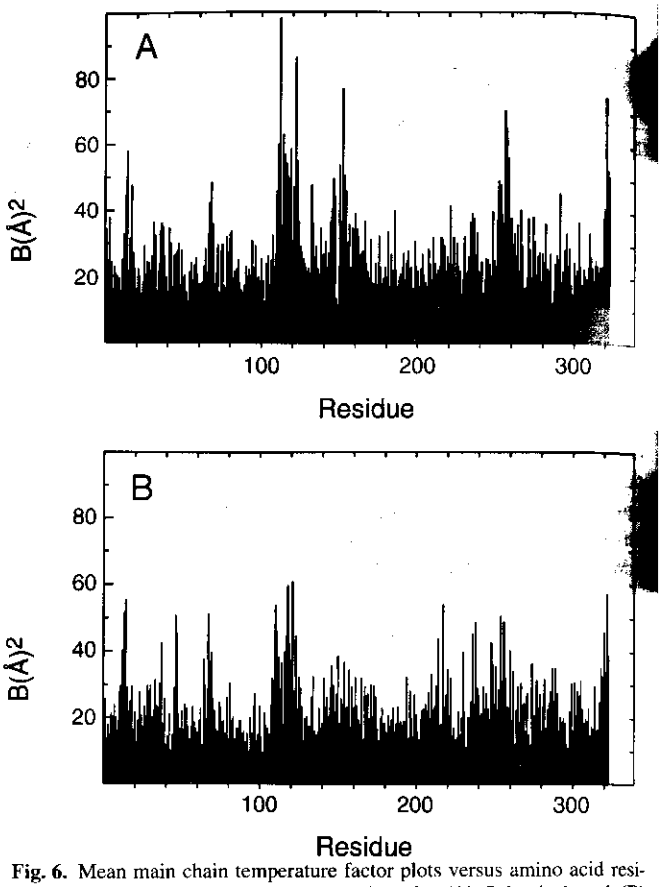

Fig. 6. Mean main chain temperature factor plots versus amino acid residue number. Shown are the mean B-values for **(A)** Subunit 1 and **(B)** Subunit 2.

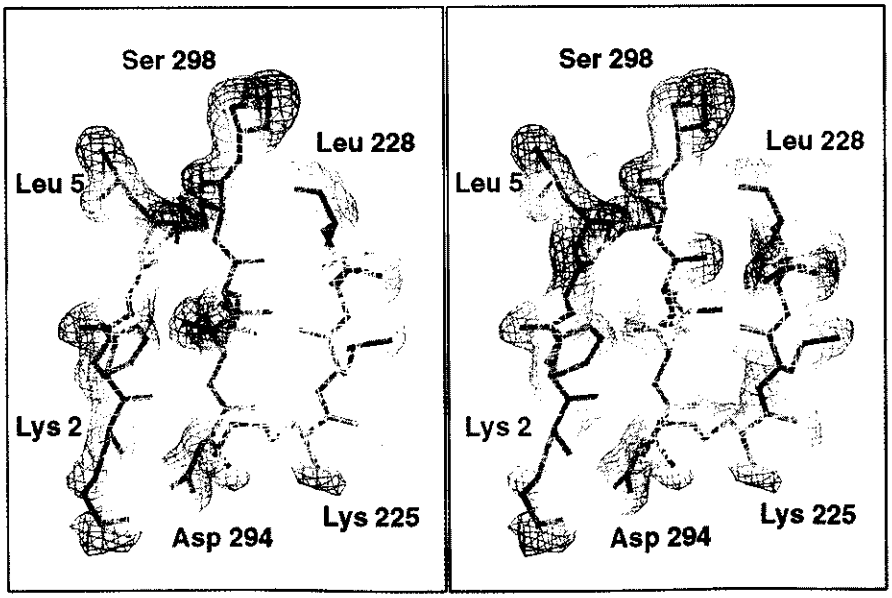

Fig. 7. Representative portion of the electron density map. This figure was prepared with the programs FRODO and FROST (Jones, 1985; Wesenberg, 1994). The electron density displayed was calculated with coefficients of the form $(2F_o - F_c)$ where F_o was the native structure factor amplitude and F_c was the calculated structure factor amplitude from the model refined at 1.95 Å resolution. The map was contoured at approximately 1σ.

space. Four of the outliers correspond to two pairs of symmetry-related residues (Asn 49 and Ala 272 in Subunits 1 and 2). Both Asn 49 and Ala 272 occur at locations where secondary structural elements cross and appear to be required for proper protein folding. The other outliers are located in reverse turns and surface loops. Plots of the mean main-chain temperature factors versus amino acid residues for both subunits are shown in Figures 6A and B. The average B-values for all backbone atoms were 29.7 Å^2 and 26.6 Å^2 for Subunits 1 and 2, respectively. A representative portion of the electron density map is displayed in Figure 7. Coordinates have been deposited in the Brookhaven Protein Data Bank (Bernstein et al., 1977) with accession number 1BSL.

Acknowledgments

This research was supported in part by grants from the NIH (AR35186 and DK47814 to I.R. and H.M.H., respectively), NSF (BIR-9317398 to I.R.) the Office of Naval Research (N00014-96-1-0087 and N00014-93-1-1345 to T.O.B.), and the Robert A. Welch Foundation (A-865 to T.O.B.). A.J.F. and J.B.T. were supported by NSRA fellowships, AR08304 and GM15950, respectively. We thank Miriam Ziegler for helpful discussions and careful review of this manuscript.

References

Anfinsen CB. 1973. Principles that govern the folding of protein chains. *Science 181*:223–230.

Baker D, Agard DA. 1994. Kinetics versus thermodynamics in protein folding. *Biochemistry 33*:7505–7509.

Baker D, Sohl JL, Agard DA. 1992. A protein-folding reaction under kinetic control. *Nature 356*:263–265.

Baldwin TO, Berends T, Bunch TA, Holzman TF, Rausch SK, Shamansky L, Treat ML, Ziegler MM. 1984. Cloning of the luciferase structural genes from *Vibrio harveyi* and the expression of bioluminescence in *Escherichia coli*. *Biochemistry 23*:3663–3667.

Baldwin TO, Shadel GS, Devine JH, Lin JW, Heckel RC. 1989. The complete nucleotide-sequence of the lux regulon of *Vibrio fischeri* and the luxABN region of *Photobacterium leiognathi* and the mechanism of control of bacterial bioluminescence. *Journal of Bioluminescence and Chemiluminescence 4*:326–341.

Baldwin TO, Ziegler MM. 1992. The biochemistry and molecular biology of bacterial bioluminescence. In: Müller F, ed. *Chemistry and Biochemistry of Flavoenzymes III*. Boca Raton, Florida: CRC Press. pp 467–530.

Baldwin TO, Ziegler MM, Chaffotte AF, Goldberg ME. 1993. Contribution of folding steps involving the individual subunits of bacterial luciferase to the assembly of the active heterodimeric enzyme. *J Biol Chem 268*:10766–10772.

Baldwin TO, Ziegler MM, Clark AC, Sinclair JF, Raushel FM, Rayment I, Holden HM, Fisher AJ, Thompson TB, Thoden JB. 1997. *Structure and folding of bacterial luciferase*. Calgary: University of Calgary Press.

Bernstein FC, Koetzle TF, Williams GJB, Meyer EF, Jr., Brice MD, Rogers JR, Kennard O, Shimanouchi T, Tasumi M. 1977. The protein data bank: a computer-based archival file for macromolecular structures. *J Mol Biol 112*:535–542.

CCP4. 1994. The CCP4 Suite: Programs for protein crystallography. *Acta Crystallogr D50*:760–763.

Choi H, Tang CK, Tu S-C. 1995. Catalytically active forms of the individual subunits of *Vibrio harveyi* luciferase and their kinetic and binding properties. *J Biol Chem 270*:16813–16819.

Clark AC, Sinclair JF, Baldwin TO. 1993. Folding of bacterial luciferase involves a non-native heterodimeric intermediate in equilibrium with the native enzyme and the unfolded subunits. *J Biol Chem 268*:10773–10779.

Cohn DH, Mileham AJ, Simon MI, Nealson KH, Rausch SK, Bonam D, Baldwin TO. 1985. Nucleotide sequence of the *luxA* gene of *Vibrio harveyi* and the complete amino acid sequence of the α subunit of bacterial luciferase. *J Biol Chem 260*:6139–6146.

Epstein CJ, Goldberger RF, Anfinsen AB. 1963. The genetic control of tertiary protein structure: studies with model systems. *Cold Spring Harbor Symposium on Quantitative Biology 28*:439–449.

Farber GK, Petsko GA. 1990. The evolution of α/β barrel enzymes. *Trends Biochem Sci 15*:228–234.

Fedorov AN, Baldwin TO. 1995. Contribution of cotranslational folding to the rate of formation of native protein structure. *Proc Natl Acad Sci USA 92*:1227–1231.

Fisher AJ, Raushel FM, Baldwin TO, Rayment I. 1995. Three-dimensional structure of bacterial luciferase from *Vibrio harveyi* at 2.4 Å resolution. *Biochemistry 34*:6581–6586.

Fisher AJ, Thompson TB, Thoden JB, Baldwin TO, Rayment I. 1996. The 1.5-Å resolution crystal structure of bacterial luciferase in low salt conditions. *J Biol Chem 271*:21956–21968.

Friedland JM, Hastings JW. 1967. Nonidentical subunits of bacterial luciferase: Their isolation and recombination to form active enzyme. *Proc Natl Acad Sci USA 58*:2336–2342.

Gething M-J, McCammon K, Sambrook J. 1986. Expression of wild-type and mutant forms of influenza hemagglutinin: The role of folding in intracellular transport. *Cell 46*:939–950.

Johnston TC, Thompson RB, Baldwin TO. 1986. Nucleotide sequence of the *luxB* gene of *Vibrio harveyi* and the complete amino acid sequence of the β subunit of bacterial luciferase. *J Biol Chem 261*:4805–4811.

Jones TA. 1985. Interactive computer graphics: FRODO. In: Wycoff HW, Hirs CHW, Timasheff SN, eds. *Methods in Enzymology 115*. New York: Academic Press Inc. pp. 157–171.

Kabsch W. 1988a. Automatic indexing of rotation diffraction patterns. *J Appl Crystallogr 21*:67–71.

Kabsch W. 1988b. Evaluation of single-crystal x-ray diffraction data from a position sensitive detector. *J Appl Crystallogr 21*:916–924.

Kraulis PJ. 1991. MOLSCRIPT: A program to produce both detailed and schematic plots of protein structures. *J Appl Crystallogr 24*:946–950.

Lee B, Richards FM. 1971. The interpretation of protein structures: Estimation of static accessibility. *J Mol Biol 55*:379–400.

Li Z, Szittner R, Meighen EA. 1993. Subunit interactions and the role of the *luxA* polypeptide in controlling thermal stability and catalytic properties in recombinant luciferase hybrids. *Biochim Biophys Acta 1158*:137–145.

Mottonen J, Strand A, Symersky J, Sweet RM, Danley DE, Geoghegan KF, Gerard RD, Goldsmith EJ. 1992. Structural basis of latency in plasminogen activator inhibitor-1. *Nature 355*:270–273.

Navaza J. 1993. On the computation of the fast rotation function. *Acta Crystallogr D49*:588–591.

Nicholls A, Sharp KA, Honig B. 1991. Protein folding and association: Insights from the interfacial and thermodynamic properties of hydrocarbons. *Proteins Struct Funct Genet 11*:281-296.

Ramakrishnan C, Ramachandran GN. 1965. Stereochemical criteria for polypeptide and protein chain conformation. *Biophys J 5*:909–933.

Rodgers DW. 1994. Cryocrystallography. *Structure 2*:1135–1140.

Rossmann MG, ed. 1972. *The Molecular Replacement Method. A Collection of Papers on the Use of Non-Crystallographic Symmetry*. New York: Gordon and Breach.

Sinclair JF, Waddle JJ, Waddill EF, Baldwin TO. 1993. Purified native subunits of bacterial luciferase are active in the bioluminescence reaction but fail to assemble into the $\alpha\beta$ structure. *Biochemistry 32*:5036–5044.

Sinclair JF, Ziegler MM, Baldwin TO. 1994. Kinetic partitioning during protein folding yields multiple native states. *Nature Struct Biol 1*:320–326.

Sugihara J, Baldwin TO. 1988. Effects of 3′ end deletions from the *Vibrio harveyi luxB* gene on luciferase subunit folding and enzyme assembly: Generation of temperature-sensitive polypeptide folding mutants. *Biochemistry 27*:2872–2880.

Teng TY. 1990. Mounting of crystals for macromolecular crystallography in a free-standing thin film. *J Appl Crystallogr 23*:387–391.

Tronrud DE, Ten Eyck LF, Matthews BW. 1987. An efficient general-purpose least-squares refinement program for macromolecular structures. *Acta Crystallogr A43*:489–501.

Waddle J, Baldwin TO. 1991. Individual α and β subunits of bacterial luciferase exhibit bioluminescence activity. *Biochem Biophys Res Commun 178*:1188–1193.

Waddle JJ, Johnston TC, Baldwin TO. 1987. Polypeptide folding and dimerization in bacterial luciferase occur by a concerted mechanism *in vivo*. *Biochemistry 26*:4917–4921.

Wesenberg G. 1994. FROST. University of Wisconsin.

Wesenberg G, Rayment I. 1995. Xcalibre. Computer program, copyright U. Wisconsin, Madison, in preparation.

Zhang X-J, Matthews BW. 1995. EDPDB: A multifunctional tool for protein structure analysis. *J Appl Crystallogr 28*:624–630.

Ziegler MM, Baldwin TO. 1981. Active center studies on bacterial luciferase: Modification with methyl methanethiolsulfonate. In: Deluca MA, McElroy WD, eds. *Bioluminescence and Chemiluminescence: Basic Chemistry and Analytical Applications*. New York: Academic Press. pp 155–160.

Ziegler MM, Goldberg ME, Chaffotte AF, Baldwin TO. 1993. Refolding of luciferase subunits from urea and assembly of the active heterodimer. *J Biol Chem 268*:10760–10765.